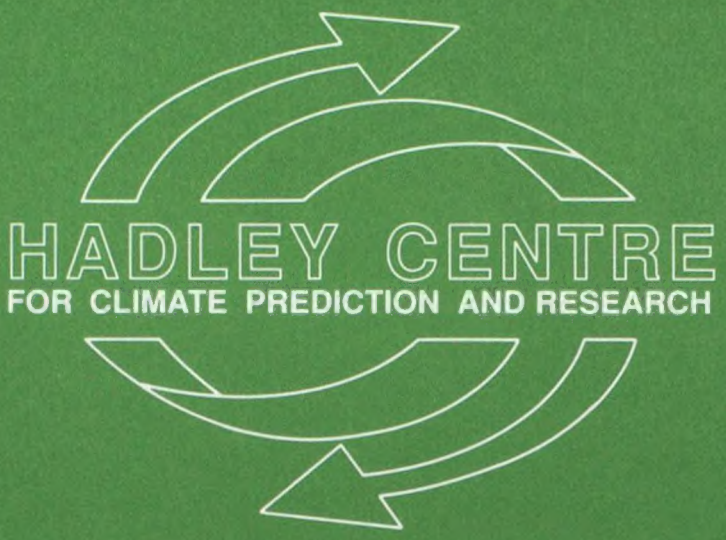

Global and regional patterns of climate change: recent predictions for the Arctic

by

P. R . Rowntree

CRTN 43

December 1993

CLIMATE
RESEARCH
TECHNICAL
NOTE

Hadley Centre
Meteorological Office
London Road
Bracknell
Berkshire RG12 2SY

CLIMATE RESEARCH TECHNICAL NOTE NO. 43

GLOBAL AND REGIONAL PATTERNS OF CLIMATE CHANGE: RECENT PREDICTIONS FOR THE ARCTIC

by

P R Rowntree

December 1993

This paper was prepared for the Proceedings of the International Conference on Global Change and Arctic Terrestrial Ecosystems (Oppdal, Norway, 21-26 August 1993)

Hadley Centre for Climate Prediction and Research
Meteorological Office
London Road
Bracknell
Berkshire RG12 2SY

NOTE: This paper has not been published. Permission to quote from it should be obtained from the Director of the Hadley Centre.

GLOBAL AND REGIONAL PATTERNS OF CLIMATE CHANGE: RECENT PREDICTIONS FOR THE ARCTIC

PETER R ROWNTREE
(Hadley Centre for Climate prediction and Research, Meteorological Office, Bracknell, ENGLAND)

ABSTRACT

The models used to estimate equilibrium and evolving changes in climate due to increases in greenhouse gas concentrations are described, with the main focus on results for the Arctic from a 75 year experiment with carbon dioxide increasing at 1% per year. The models suggest that temperatures will increase generally, but with large spatial variations which differ considerably between models. Precipitation including winter snowfall is generally increased in amount but, for a given mean fall, decreases in frequency. Because of increases in evaporation, soil moisture is decreased in many areas in summer but increases through the rest of the year. Changes in circulation significantly modify these general statements on a regional scale.

There are important uncertainties concerning the future (and also past) changes in radiative forcing including the effects of sulphate aerosols. Uncertainties with the model include the ocean simulation and the representations of clouds and land surface evaporation. However, evidence from observations encourages some credence in the predictions, at least on the larger scales.

THE GREENHOUSE EFFECT

The greenhouse effect is not new. It has been keeping the Earth warm since its formation. In geologically recent times the most important greenhouse gases have been water vapour and carbon dioxide (CO_2). In the absence of greenhouse gases, the heating by incoming solar radiation must be balanced by longwave radiation emitted from the earth's surface. If we know the reflectivity of the earth for solar radiation - it is about 30% at present - we can calculate the temperature of the Earth's surface needed to give this balance to be about -18°C or 255K. With greenhouse gases present, the longwave radiation from the surface is partly absorbed and then re-emitted by the gases at the temperature of the air at their level. This has the effect of raising the level from which radiation is effectively emitted to space to several kilometres above the surface, where the temperature is about 30K lower than that near the surface. Consequently, the surface temperature can be higher by about this amount and

the Earth will emit the same amount of radiation to space as in the absence of greenhouse gases.

The concentrations of several greenhouse gases are observed to be increasing. CO2, methane, nitrous oxide and several chlorofluorocarbons (CFCs) have all increased since the start of the industrial era. However, it is also believed that the amount of sulphate aerosols in the atmosphere has increased so increasing its reflectivity for solar radiation - though this is difficult to measure. Also, stratospheric ozone, a greenhouse gas, has been depleted over the last 20 years or so due to the increases in CFCs. Its effect is thought to be perhaps as large as that due to the CFCs and of opposite sign (Isaksen et al. 1992). Measurements of air in ice cores, supported by late 19th century observations, suggest that since the start of the industrial era in about 1750, the largest contribution, about 1.5 W m^{-2} so far in terms of its effect on longwave radiation at the top of the troposphere, has come from CO_2. Methane and nitrous oxide have together contributed another 0.5 W m^{-2}, whilst a "best estimate" of the opposite effect of aerosols is also about 0.5 W m^{-2}. Volcanic eruptions, such as that of Mt. Pinatubo in 1991, are thought to have significant shortterm effects on global mean temperature; however, they are not expected to induce longterm change unless there is a major change in their frequency or intensity.

MODELLING CLIMATE CHANGE DUE TO THE GREENHOUSE EFFECT

Climate models: To predict the effects of increasing CO_2 and other trace gases on climate, it is necessary to use a climate model based on the relevant physical equations. In "finite difference" models, such as that used at the Meteorological Office (MO), the temperatures, winds or currents and other variables in the atmosphere and ocean are represented for a three-dimensional array of boxes. In the horizontal, the gridbox array follows lines of constant latitude and longitude, while in the vertical there are typically 10 to 20 layers in both atmosphere and ocean. Because of the large computing requirements, the horizontal grid length used in CO_2 experiments to date has been limited to about 2.5 degrees of latitude; Gates et al. (1990) found that, with this resolution, quite a realistic simulation of the atmospheric circulation was obtained. With coarser resolution, major errors were evident in the simulated circulation patterns (see Fig. 4.1 in Gates et al.). However, the ocean simulation at 2.5 degrees latitude is quite poor, typical horizontal scales being less in the ocean than in the atmosphere; it is clear that in future the ocean model will need to be on a finer mesh.

Climate predictions: To make a climate simulation, the procedure is much as in a numerical forecast, the equations representing the atmospheric physics being integrated forwards in time. After 5 days the accuracy of prediction of individual events is deteriorating; however if the model is run further, its anticyclones and depressions should continue to develop and move in a realistic fashion, and by running the model on for many years a simulation of climate can be obtained. To estimate the effect of a change in forcing, the relevant parameter (e.g. the amount of CO_2) is changed and the simulation is repeated with this change.

Equilibrium and transient response experiments: Results obtained from climate models over the last decade have been from two types of experiment, commonly called equilibrium experiments and transient response experiments. The equilibrium experiments are intended to estimate the equilibrium response to an increase (usually a doubling) of CO_2. Because of the large amount of computing that would be needed to take a model with a deep ocean to equilibrium, they usually use a "slab" ocean model consisting of a mixed layer 50m thick with no currents but sufficient thermal inertia to represent the seasonal variation. The advection of heat in this slab model is represented by a prescribed seasonally varying "flux correction" by which energy is input to the ocean so as to maintain realistic temperatures and sea-ice distributions in a longterm climatological sense. In any perturbation experiment, for example with CO_2 doubled, the same flux correction as calculated for the control experiment is applied.

The "transient response" experiments use a model with a deep ocean to predict the evolving response to gradually increasing greenhouse gases. Thus ocean currents are represented including vertical motion on the gridscale and subgridscale convective and diffusive mixing which disperse the effects of surface fluxes of heat, water and momentum throughout the ocean.

MODELS

As discussed by Gates et al. (1992) in the 1992 IPCC (Intergovernmental Panel for Climate Change) Report, four coupled models of the atmosphere and deep ocean have been used to study the transient response to increasing greenhouse gases - from the Geophysical Fluid Dynamics Laboratory (GFDL) at Princeton, USA (Manabe et al. 1992), the National Center for Atmospheric Research (NCAR) at Boulder, USA (Meehl et al 1993), the Max Planck Institute (MPI) at Hamburg, Germany (Cubasch et al. 1992) and the Meteorological Office (MO) at Bracknell, UK (Murphy 1992).

Table 1: Structure of four models used for transient response experiments (see text for explanation and references)

Model	GFDL	NCAR	MPI	MO
Atmosphere				
Horizontal resolution[1]	R15	R15	T21	2.5°*3.75°
Layers	9	9	19	11
Ocean				
Horizontal resolution[1]	4.5°*3.75°	5°	4°	2.5°*3.75°
Layers	12	4	11	17
Greenhouse gas scenario				
CO_2 increase (/year)[2]	1%	1%	IPCCA	1%
CO_2 doubling time (yr)	70	100	60	70

Notes: [1]: R15 and T21 indicate spectral resolutions (see text) (R = Rhomboidal and T = Triangular). For the non-spectral representations, the first figure is the latitudinal, the second the longitudinal resolution - only one figure is given if both are the same.

[2]: 1% compound for GFDL and MO, 1% simple for NCAR. "IPCCA" refers to the Scenario A (also called "Business as usual") used in the 1990 IPCC Report (Houghton et al. 1990)

The structure of these models is indicated in Table 1. Note that three of the models use a spherical harmonical (or "spectral") representation of the atmosphere for advection. The atmospheric physics is computed on a 4.5° by 7.5° grid for the R15 models, and a 5.6° by 5.6° grid for the T21 spectral resolution. The models were run both with constant CO_2 (the control experiments) and with gradually increasing CO_2. Except for the NCAR model all were run to the time of doubling of CO_2 or beyond. Meehl et al. (1992) report results for the NCAR model to Year 60.

An increase of 1%/year is faster than the observed past rate of increase for CO_2 which has risen from about 0.3%/year in the 1960s to nearly 0.5%/year in the 1980s; thus the accumulated increase over the 1960-90 period is equivalent to about 12 years at 1%/year. Earlier increases starting from about 1750 were slower though not negligible. As discussed earlier, the globally averaged changes in radiative forcing due to other trace gases and aerosols may have been roughly in balance over recent decades, though their regional effects probably have not due to the uneven distribution of sulphate aerosols.

Most of the results discussed here will be from the MO model, which is described in more detail below, with comparisons to results from other coupled models where available. This is a significant limitation; in particular, the effects on pressure at mean sea level (PMSL) are only available for the MO model. However, as noted earlier, the relatively low horizontal resolution provided by R15 or T21 spectral models does not allow as realistic simulations of the circulation as can be obtained with the grid used in the MO model, especially in high latitudes, so the MO model may provide the best guidance on circulation changes.

The Meteorological Office (MO) model: The MO atmospheric model used in the experiments discussed here is a development of that assessed in the 1990 IPCC Report by Gates et al. (1990). As indicated in Table 1, it represents the surface pressure, and the temperature, humidity and wind components on 11 layers on a 2.5 by 3.75 degree latitude-longitude mesh. The deep ocean model has temperature, salinity and currents on 17 layers and the same horizontal mesh as the atmospheric model. A flux correction is still needed to maintain a realistic climate, though the temperature errors without it are smaller than in the equilibrium experiment with the slab model. There is an assumption implicit in the use of the flux correction technique that the errors in the simulations of the two climates are similar. This is a useful first approximation to estimation of the errors, though it is likely to become increasingly invalid as the differences between the ocean circulations in the control experiment and the perturbation experiment increase.

The land surface is represented by a model with the same horizontal mesh as the atmosphere. Fourteen surface and subsurface characteristics are defined as a function of the soil and vegetation types for each gridbox which are specified from the 1° data sets constructed by Wilson and Henderson-Sellers (1985). The soil is represented by four layers for thermal processes and one layer plus a canopy water store for hydrological processes.

Validation of MO control experiment: As shown by Gates et al. (1990), the MO model simulates the atmospheric simulation in a generally realistic manner. For sea level pressure (Fig. 1), the major observed features are present in winter - the Aleutian and Icelandic lows and a high over Siberia with a ridge across the east Siberian Arctic Ocean to link with a north-south ridge over Canada. However, the trough along the north coast of western Eurasia is weaker than observed. In summer, the observed pattern shows a weak circumpolar trough near 60N, with

minima near Labrador and the east Atlantic, while over Siberia this trough becomes an extension of the Asian summer low. There is a weak high near the pole. The model captures these features though there is no clear east Atlantic low. However, the high over the Arctic Ocean is too strong, being 6 to 8 hPa above the minima near 60N compared with an observed excess of about 4hPa.

The simulated precipitation (not shown) at Years 66-75 of the control experiment is generally similar to that shown by Gates et al. (1990) and includes the main observed features. In winter, precipitation north of 60N is less than 1 mm/day except over the southern half of Alaska and adjacent parts of northwest Canada, and over Scandinavia. In summer, precipitation exceeds 1 mm/day over all Arctic land in the MO model and, except some northern coastal areas, in the observed. The model has an area exceeding 2 mm/day extending north to 65-68N over Eurasia and to near 60N over N America. This is more extensive than in the model shown in Gates et al., making it more realistic over much of Eurasia, but less so over N America.

RESULTS

Temperature changes: The annually averaged temperature changes in transient response experiments have been shown by Gates et al. (1992). The responses obtained from these experiments at the time of doubling of CO_2 are similar in many ways to those from equilibrium experiments (Mitchell et al, 1990) but there are important differences, in part due to the inclusion of the deep ocean and ocean currents; this allows representation of the vertical mixing which slows the response of the ocean, so that by the time of doubling at 1%/year (typical of the rates to be expected in the next few decades) the global mean warming is only about 60-70% of the equilibrium figure, and the warming of the oceans is generally less than that of the land. Parts of the ocean with deep mixing in winter, notably the Antarctic Ocean and the North Atlantic Ocean, are particularly slow to warm. In the Hadley Centre experiment (Fig. 2), some small regions of cooling in both areas still persist at Years 66-75 (when CO_2 is doubled) when the mean land surface warming is about 3K (or degree C) compared with 1.5K for the ocean. In contrast, in equilibrium experiments, the high latitude oceans could display some of the largest temperature rises (e.g. Bretherton et al (1990), Fig 6.5(b)).

The typical magnitudes of warming for different surfaces may be ordered from large to small in each season as shown in Table 2. In summer the greatest warming occurs over those land areas which have less snow (e.g. the Canadian Archipelago) as a result of the climate change. Warming

is almost as large over those parts of the land which are drier as a result of the increase in CO_2 and are so dry as to limit evaporation (and so the evaporative cooling); mostly, such areas are south of 60N in the model. In winter regions with sea-ice show the largest warming, but in summer sea-ice regions are second only to the more deeply-mixed oceans for their lack of warming. This is because the sea-ice surface is already at melting point most of the summer in the control experiment and though it absorbs more heat due to a longer melt season, it cannot warm further till the ice is melted; even then the large thermal inertia of the ocean allows only slow warming. The effects of the extra heat gained in summer on surface temperature show in autumn and winter when ice is thinner and less extensive, with the largest warming over areas where the ice extent is much reduced with increased CO_2, such as the Barents Sea, Bering Strait and Sea of Okhotsk.

Table 2: Ordering of typical temperature changes from highest to lowest with typical changes (K) at Year 66-75 of the MO experiment in middle and high northern latitudes

	Typical change
For winter:	
melted sea-ice	about 10
other sea-ice	+4 - +8
melted snow	+4 - +8
most land	+3 - +6
land with ocean/ice to windward	-1 - +4
most ocean	+1 - +2
ocean with deep mixing	-1 - 0
for summer:	
melted snow	+4 - +7
dried land	+3 - +6
most land	+2 - +4
land with ocean/ice to windward	+1 - +3
most ocean	+1 - +3
sea-ice	+0 - +1
ocean with deep mixing	-1 - +1

Interactions between temperature and circulation changes: The atmospheric circulation can be substantially modified by spatial variations of the warming (Fig. 3). One example is a general reduction of pressure over the summer continents; this corresponds to the greater warming of the continents than of the oceans and represents an intensification of the continental lows associated with the summer monsoon. A less obvious example pointed out by Hall et al. (1993) is that the reduced baroclinic gradient over the west Atlantic associated with the large winter

warming over eastern Canada weakens the storm track in this region, while the cooling near southern Greenland enhances baroclinicity further east. This, together with the effects of a moister atmosphere increasing the potential for latent heat release in storms, leads to a downstream intensification of the storm tracks and associated westerly winds. In the MO model, this generates an increased westerly flow in autumn and winter over the N Atlantic sector and northern Eurasia south of a fall of pressure over the Arctic.

Some aspects of the climate change are thus of a regional nature and can be attributed to changes in wind direction etc. For example, Fig. 2 shows a warming of up to 5K over Scandinavia in winter, which is likely to be due in part to increased westerly component from the warm ocean to the west. On the other hand over the Pacific coasts of eastern Alaska and western Canada, where a reduction of northward flow weakens warm air advection, there is cooling or only slight warming, though part of this may be due to the small warming of the ocean to windward (SW). This feature is particularly strong in this decade; averages for Years 31-70 show a warming of 0-1K and PMSL changes only half as large though of similar pattern. In summer, the largest warming over northern Asia is in the sector (60-100E) affected by increased southerly flow from warmer regions around an increase in pressure near Severnaya Zemlya. These circulation changes, while not likely to be correct in detail, are indicative of the type of regional effects to be expected with greenhouse warming.

Precipitation changes: With enhanced CO_2, precipitation increases generally in winter over land north of 45N and over most of the Arctic land areas in summer (Fig. 4). One of the few exceptions north of 60N at Years 66-75 is in the Ob-Yenisei basins in summer; the long period (Year 31-70) mean shows a similar but weaker decrease in this region, with a break near 65N. As discussed above, the PMSL difference charts show this to be a region with either higher pressure or increased flow from the arid regions to the south; this feature is also less pronounced in the 40 year mean. Precipitation is also decreased over the Pacific coastal areas of eastern Alaska and northwest Canada and over southern Greenland. These regions are adjacent to seas where warming is particularly limited by the deep mixing of the oceans and, at least in the Atlantic, the weakening of the thermohaline circulation which transports warm water northward. The general rise in atmospheric water vapour content, which is mainly responsible for the increases in precipitation is likely to be weak or absent in these regions. The increases in precipitation in summer near Hudson's Bay, Scandinavia and

east and west of the Bering Strait are all associated with falls of pressure of 1hPa or more.

Soil Moisture: With such general increases in precipitation, one might expect a widespread increase in soil moisture. However, equilibrium experiments have shown rather consistently (Mitchell et al. 1990; Fig 5.8) that soil moisture is predicted to decrease over middle and high latitudes in summer. The main reason for this, at least where the rainfall changes are small, is that evaporation is predicted to increase from spring onwards due to earlier snowmelt and to the effect of higher temperatures on the evaporation through the Clausius-Clapeyron relation (e.g. see Rowntree 1991). In the MO transient response experiment (Fig. 5), summer soil moisture north of 60N is increased only where rainfall is increased by more than 0.2 mm/day. This is consistent with the changes in evaporation (not shown) which are typically an increase of about 0.25 mm/day in the June-August mean. Elsewhere there are decreases which are mostly less than 1cm north of 60N but reach 2 cm where rainfall is decreased in the Ob basin in this decade; this peak decrease is only 1cm in the Year 31-70 mean.

There is little consistent increase in the soil moisture differences after Years 31-40; the same applies to the changes in precipitation and PMSL; the explanation is believed to be the similarity of the land-ocean temperature contrasts through this period. This is discussed further in the section on "Comparison of transient experiment results for Arctic land". The Years 31-70 seasonal mean soil moisture differences (not shown) reveal that soil moisture is increased over most regions north of 60N in autumn and spring as well as winter due to increased rainfall throughout the year.

Changes in intensity of precipitation: Analysis of the results over Europe (J Gregory, personal communication) from the equilibrium experiment UKHI used in Mitchell et al. (1990) has shown that in the warmed CO_2 climate, for a given average rainfall, the rainfall tends to be more intense with, for example, the rainfall on the wettest day of the season generally increasing more (or decreasing less) than the mean rainfall. This is presumably because of the greater water content of warmer air. Consistently with this, the percentage of dry days commonly increases relative to the mean rainfall. The year to year variability (seasonal SD) also generally increases more than the mean. The original analysis was confined to mid-latitude regions of Europe. However, the analysis of dry day frequency has been repeated for the summer season (June-August) of the last 10 years of the transient experiment, using a criterion for a dry day of less than

0.05 mm. Fig. 6 (J Gregory, personal communication) shows that most Arctic land areas have more dry days, including much of the region with more rainfall.

Snowfall and snowmass changes: The modelled snow cover is generally realistic in the model. Gates et al (1990) show this for N America with the 1cm liquid water equivalent contour close to the observed 5cm snowdepth contour, indicating correct snowdepth if the snow density is 0.2 g/cm^3. They noted that results were similar over Europe and western Asia, but that snow was too extensive over eastern Asia. In the MO transient response experiment (not shown) the 1cm snowmass contour over N America in the December-February mean is similarly located. Over coastal eastern Asia, it extends south to about 40N, which appears to be realistic as Matson et al. (1986) show continuous cover north of about 45N in winter and 25% frequency at about 40N, where snowfalls are heavy when they do occur.

Over northern Asia, the modelled snowmass exceeds 50 kg/m^2 in winter. In the June-August mean, the 10kg/m^2 contour is mostly near 70N except at 60-80E where it is near 65N. South of here, the snowfree season must end by June 1 or very soon after. Lydolph (1977) shows a map of date of disappearance of snowcover; the June 1 contour is near 70N from 100-160E, with a lower latitude further west reaching about 66N at 60-80E. This comparison indicates that the summer snowcover has realistic extent in the model over the Asian Arctic. A similar comparison with the corresponding map for N America in Hare and Hay (1974) indicates comparable quality in that region, the model capturing the NW-SE alignment of the early June snow margin from northern Alaska to central Hudson's Bay.

The increase in CO_2 reduces winter snow mass (Fig 7) over most regions south of 60N, and also over regions of Scandinavia and southern Alaska north of this latitude. Most of the rest of the Arctic land has increased snow mass in this season, with increases exceeding 20 kg/m^2 northwest of Hudson's Bay and in the northern parts of the Ob and Yenisei basins. In these regions of increased snowmass the increase in precipitation has more effect on the snow budget than the later start to the snow season. The differences in snowfall rate in winter (Fig 8) show that a much more extensive area has increased snowfall in association with the increased total precipitation. This area includes most of the land areas with a persistent winter snowcover except the Pacific coast regions of Alaska and western Canada and southern Greenland, which areas have less total precipitation as discussed earlier.

In summer, snowfall and snow mass are decreased over

virtually all northern hemisphere land except the central and eastern parts of Greenland. The snowmass changes over Greenland are much larger than elsewhere because, being permanent snow, the changes have accumulated over 70 years from the start of the experiment. It is interesting that the regions of Greenland which are warmed least also have less snowfall and so lose snowmass, while the regions which warm most gain snow mass. The same happens over Antarctica.

COMPARISON OF TRANSIENT EXPERIMENT RESULTS

As discussed earlier, four experiments were compared by Gates et al. (1992), run using the NCAR, GFDL, MPI and MO models. Averages were shown for about the time of doubling, except that the NCAR run was for about a 45% increase, when the equilibrium warming would be just over half that at the time of doubling (over half because of the logarithmic relation between temperature increase and CO_2 increase).

Only annual mean temperature changes were shown for the experiments, but there is additional information available, mostly in the papers on the results referenced earlier.

Table 3: Range (Rnge)and estimated average (Avge) of annual mean temperature (K) differences (IPCC, 1992) (NCAR values doubled - see text)

	GFDL		MPI		NCAR		UKMO	
	Rnge	Avge	Rnge	Avge	Rnge	Avge	Rnge	Avge
Arctic Oc	4-6	5	4-8	6	1-5	3	3-7	5
Land 60N	2-5	3.7	1-3	1.9	1-4	2.4	1-5	3.9
Ocean 60N	1-4	3.2	0-2	1.2	1-4	3.1	-1-4	1.2
Land 30N		3.1		1.9		1.1		2.7
Ocean 30N		2.3		1.1		1.3		2.0
Ocean 0N	1-3	1.9	1-2	1.5	1-2	1.2	1-2	1.3

Differences in averages between regions (AOc = Arctic Ocean)

	GFDL	MPI	NCAR	UKMO
AOc-Land 60N	1	4	0.6	1
AOc-Ocn 60N	2	5	0	4
Land-Ocn 60N	0.5	0.7	-0.7	2.7
Land-Ocn 30N	0.8	0.8	-0.2	0.7

Table 3 shows estimated annual mean temperature changes for selected regions and differences between the regions.

The NCAR differences have been doubled to allow for the smaller CO2 increase. There are large differences between the patterns of warming in the different experiments. The NCAR model is quite distinct with little difference between the warming over the Arctic Ocean and that at 60N. However, although the other models have a similar overall gradient between the Arctic Ocean and the equator (3.2-4.7K), they differ markedly in its distribution. For example, comparing the MO and GFDL models, they have similar gradients between the Arctic Ocean and 60N over land, but the MO model has a much smaller warming over the ocean at this latitude, and so a larger north-south gradient between there and the Arctic Ocean. The MPI model has a gradient of this size or greater over both ocean and land.

The ocean-land contrast at 60N is much larger in the MO model than in the others. This is likely to be important in generating ocean-land contrasts in atmospheric variables. An interesting feature of the MO results is that after the first 30 years clear patterns of precipitation and circulation change have developed in the MO model which then persist with little further amplification through the next 40 years. These features appear to be associated with the development of the ocean-land contrasts which show a similar temporal evolution. The weakness of these ocean-land contrasts in the other models may explain the fact that similar temporal behaviour is not obvious in other models; for example, the GFDL soil moisture differences shown by Gates et al (1992) and Manabe et al. (1992) increase rather steadily from years 40-60 to 80-100. The reasons for the large ocean-land contrast in the MO model are not fully known, though Murphy (1992) has suggested a role for cloud feedbacks over land, with the warming reducing the cloudiness there and so intensifying the warming.

The soil moisture differences at about the time of doubling of CO_2 can also be compared. These are similar in the GFDL model to those already discussed for the MO model, with decreases predominant in summer and increases in winter over Arctic land. The MPI model has a similar but smaller seasonal variation in the effects of CO_2 on soil moisture. In particular, the summer drying is much less widespread. All the models tend to have more precipitation in the Arctic in winter; in summer, patterns are patchy with the MO model showing the most consistent increases over Arctic land.

UNCERTAINTIES

There are important uncertainties in these results. Major ones include:

(a) radiative forcing - as discussed earlier, the forcing of the climate system by changes in the environment is imperfectly known. This problem is not confined to predicting future greenhouse gas concentrations; sulphate aerosols are thought to be important in compensating the warming due to greenhouse gases but they are only just being included in the climate models and their past as well as their future concentrations are still uncertain. Evidence so far indicates that the predictions of warming omitting aerosol effects may be too large particularly in the regions of large emissions and immediately downwind. Interestingly just as the effects are being recognised, they are decreasing in two of the most important areas, Europe and N America, as fuel use turns increasingly to less sulphurous forms. If such a decrease is of global scale and the effects have been large, one may expect an acceleration of warming in the immediate future as the braking effect of aerosols is reduced.

(b) the ocean model - the flux corrections applied to keep the ocean temperatures and salinities near to reality are significant fractions of the actual fluxes suggesting that the modelled changes in temperature and salinity due to the ocean currents are too small.

(c) the representation of cloud-radiation interactions - sensitivity to this was highlighted by a series of experiments in which global mean warming ranged from 1.9 to 5.2K for doubled CO_2, depending on which of three cloud representations was used (Senior and Mitchell 1993).

(d) the representation of the land surface hydrology - one improvement needed is to make the resistances imposed by plant stomata dependent on atmospheric variables such as temperature, vapour pressure deficit below saturation and solar radiation, as well as increased CO2. An increase in evaporation as the climate warms is likely to be reduced by these dependences; they are now being included in the MO model.

POSSIBLE INTERACTIONS WITH BOREAL FORESTS

One of the main climate changes predicted as a consequence of increased greenhouse gases is a warming of high latitude land. This may be expected to favour changes in vegetation, such as a contraction of the tundra region, and a northward shift of boreal forest. There is a possibility of a feedback on such changes due to the lower albedos of forested than deforested regions both in the snowfree season when coniferous forest has typical albedos of 0.12, a few per cent below that of tundra and deciduous forest, and more importantly in the presence of snow when the masking of the snow cover by trees can reduce albedos

by up to about 60% compared with exposed snow (Robinson and Kukla 1985; Thomas and Rowntree 1992; Bonan et al 1992). Using a slab model of the ocean, Bonan et al found a large cooling of the climate in middle and high latitudes when boreal forest was removed. The zonal averages of temperature changes over land near 60N reached 12K in April, and 5K or more in other mid-season months. Thomas and Rowntree (1992) obtained smaller changes partly because ocean surface temperatures were kept the same, and partly because they deforested a smaller area.

Provided soil conditions are favourable the forest may spread north faster than it is eroded on the south side in which case the tree belt would widen and so provide a positive feedback to warming. On the other hand a negative feedback is possible if the forest is eroded on the south side by either onset of a warmer less favourable climate or by man's activities and does not advance as quickly northward because soils are unsuitable.

VALIDATION

Validation of the model's global mean temperature predictions is difficult because of the wide range of model sensitivities (e.g. the sensitivity to different cloud representations discussed above), the uncertainty in the total changes in greenhouse forcing to date and the influence of natural variations of the climate. If only the enhancements of the greenhouse effect are considered, the observed warming of about 0.5K over the last century (Folland et al. 1990) fits best with the least sensitive of Senior and Mitchell (1993)'s experiments, which found a 1.9K response of global mean temperature for a doubling of CO2. However, if the contributions of decreased ozone and increased sulphate aerosol have been as important as suggested in the 1992 IPCC Supplement (Isaksen et al., 1990), a greater sensitivity is needed to fit the observed record. Natural variations introduce a similar uncertainty: in their absence, the observed warming might have been either larger or smaller, implying a larger or smaller sensitivity.

Validation of regional effects is at an early stage. Comparison of the spatial pattern of warming in the 1980s relative to the preceding 30 years with model predictions (Gates et al. 1992 (Fig B4), Folland et al. 1992 (Fig C5)) shows some marked similarities, notably in the strong warming over the northern continents, and the cooling near southern Greenland.

SUMMARY AND CONCLUSIONS

The conclusions of this paper may be summarised as below.

1. The predictions of climate change over Arctic land in the MO model show the following features:

a. Temperatures increase generally, but with a wide range of magnitudes - most over melted snow, least over land with ocean or sea-ice to windward, especially where the ocean warming is small.
b. In all seasons precipitation increases over most of the area; for a given mean rainfall, intensity, at least in summer, tends to increase, and frequency to decrease. Soil moisture increases generally except in summer.
c. Snowfall increases in winter over most of the Arctic; snowmass increases over a smaller area; snowfall and snowmass decrease in summer except over parts of Greenland.
d. Circulation changes forced by spatial variations in warming are responsible for regional features including decreases in precipitation and relatively weak warming, and other exceptions to the above general statements.

2. Comparison of the four available transient response experiments reveals large differences in the gradients between the Arctic Ocean and 60N and the ocean-land contrast at 60N.

3. There are important uncertainties associated with the radiative forcing including the effects of sulphate aerosols, with ocean simulation, with cloud representations and with land surface hydrology. However, evidence from observations encourages some credence in the predictions, at least on the larger scales.

4. As vegetation responds to any change in climate, there is a possibility of important feedbacks due to changes in the extent of masking of highly reflective snow.

ACKNOWLEDGMENTS

The Hadley Centre 75-year transient response experiment which supplied many of the results reported here was supported by the Department of the Environment.

REFERENCES

Bonan, G.B., D. Pollard and S.L. Thompson, 1992. Effects of boreal forest vegetation on global climate. Nature, 359, 716-718.

Bretherton, F.P., K. Bryan and J.D. Woods, 1990. Time-dependent greenhouse-gas-induced climate change. In: Climate change: the IPCC scientific assessment, (Houghton J.T., Jenkins G.J. and Ephraums, J.J., Ed.), Cambridge University Press, 173-193.

Cubasch, U., K. Hasselmann, H. Hock, E. Maier-Reimer, B.D. Santer and R. Sausen, 1992. Time-dependent greenhouse warming computations with a coupled ocean-atmosphere model. Climate Dynamics, 8, 55-69.

Folland, C.K., Karl, T.R., Nicholls, N., Nyenzi, B.S., Parker, D.E. and Vinnikov, K.Ya., 1992. Observed climate variability and change. In: Climate change 1992: the supplementary report to the IPCC scientific assessment (Houghton, J.. T., Callander, B.A. and Varney, S.K., Ed.). Cambridge University Press, 135-170.

Folland, C.K., Karl, T. and Vinnikov, K.Ya., 1990. Observed climate variations and change. In: Climate change: the IPCC scientific assessment, (Houghton J.T.., Jenkins G.J. and Ephraums, J.J., Ed.), Cambridge University Press, 195-238.

Gates, W.L., Mitchell, J.F.B., Boer, G.J., Cubasch, U. and Meleshko, V.P., 1992. Climate modelling, climate prediction and model validation. In: Climate change 1992: the supplementary report to the IPCC scientific assessment (Houghton, J.T., Callander, B.A. and Varney, S.K., Ed.). Cambridge University Press, 97-134.

Gates, W.L., P.R. Rowntree and Q-C. Zeng, 1990. Validation of climate models. In: Climate change: the IPCC scientific assessment, (Houghton J.T., Jenkins G.J. and Ephraums, J.J., Ed.), Cambridge University Press, 93-130.

Hall, N.M.J., B.J. Hoskins, P.J. Valdes and C.A. Senior, 1993. Storm tracks in a high resolution GCM with doubled CO_2. Accepted for publication in Q. J. R. Meteorol. Soc.

Hare, F.K. and J.E. Hay, 1974. The climate of Canada and Alaska. In Climates of North America (Ed. R.A. Bryson and F.K. Hare). World Survey of Climatology. Volume 11. Elsevier Scientific Publishing Company, 420 pp.

Houghton, J.T., G.J. Jenkins and J.J. Ephraums (Editors), 1990. Climate Change. The IPCC scientific assessment, Cambridge University Press, 365 pp.

Isaksen, I.S.A., Ramaswamy, V., Rodhe, H. and Wigley, T.M.L., 1992. Radiative forcing of climate. In: Climate change 1992: the supplementary report to the IPCC scientific assessment (Houghton, J.T., Callander, B.A. and Varney, S.K., Ed.). Cambridge University Press, 47-67.

Lydolph, P.E., 1977. Climates of the Soviet Union. World Survey of Climatology, Vol. 7. Elsevier Scientific

Publishing Company. 443 pp.

Manabe, S., M.J. Spelman and R.J. Stouffer, 1992. Transient responses of a coupled ocean-atmosphere model to gradual changes of atmospheric CO2. Part II: seasonal response. J. Climate, 5, 105-126.

Matson, M., C.F. Ropelewski and M.S. Varnadore, 1986. An atlas of satellite-derived northern hemisphere snow cover frequency. NOAA Atlas. U.S. Dept. of Commerce.

Meehl, G.A., W.M. Washington and T.R. Karl, 1993. Low-frequency variability and CO_2 transient climate change. Part 1. Time-averaged differences. Climate Dynamics, 8, 117-133.

Mitchell, J.F.B., S. Manabe, T. Tokioka and V. Meleshko, 1990. Equilibrium climate change. In: Climate change: the IPCC scientific assessment, (Houghton J.T., Jenkins G.J. and Ephraums, J.J., Ed.), Cambridge University Press, 131-164.

Murphy, J.M., 1992. A prediction of the transient response of climate, Climate Research Technical Note 32, Meteorological Office, Bracknell, UK.

Robinson, D.A. and G. Kukla, 1985. Maximum surface albedo of seasonally snow-covered lands. J. Climatol. Appl. Meteorol., 24, 402-411.

Rowntree, P.R., 1991. Atmospheric parametrization schemes for evaporation over land: basic concepts and climate modelling aspects. In: Land surface evaporation: measurement and parametrization (Schmugge, T.J. and Andre, J-C., Ed.), Springer-Verlag, New York, 5-29.

Senior, C. A. and J.F.B. Mitchell, 1993. CO2 and climate; the impact of cloud parametrizations. J Climate, 6, 393-418.

Thomas, G. and P.R. Rowntree, 1992. The boreal forests and climate. Q. J. R. Meteorol. Soc., 118, 469-497.

Watson, R.T., H. Rodhe, H. Oeschger and U. Siegenthaler, 1990. Greenhouse gases and aerosols. In: Climate change: the IPCC scientific assessment, (Houghton J.T., Jenkins G.J. and Ephraums, J.J., Ed.), Cambridge University Press, 1-40.

Wilson, M.F. and A. Henderson-Sellers, 1985. A global archive of land cover and soil data for use in general circulation climate models. J. Climatology, 5, 119-143.

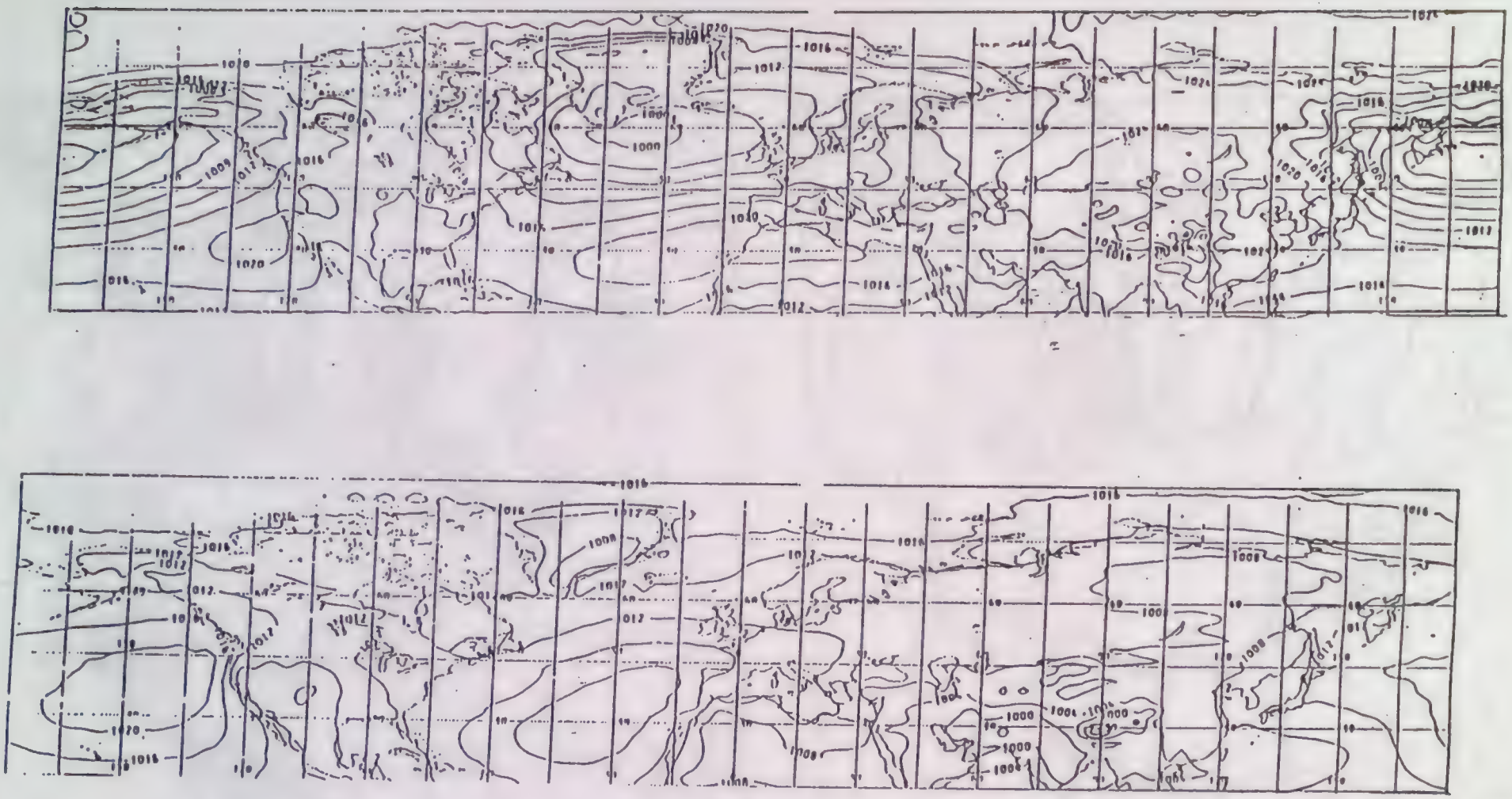

FIG.1. Modelled sea level pressure for Years 66-75 of control experiment

December-February (above), June-August (below).

Fig. 2. Unit K.

SURFACE TEMPERATURE DIFFERENCE for DJF
transient coupled model: anomaly – control (yrs 66 to 75)
contours at intervals of 1
shading where negative

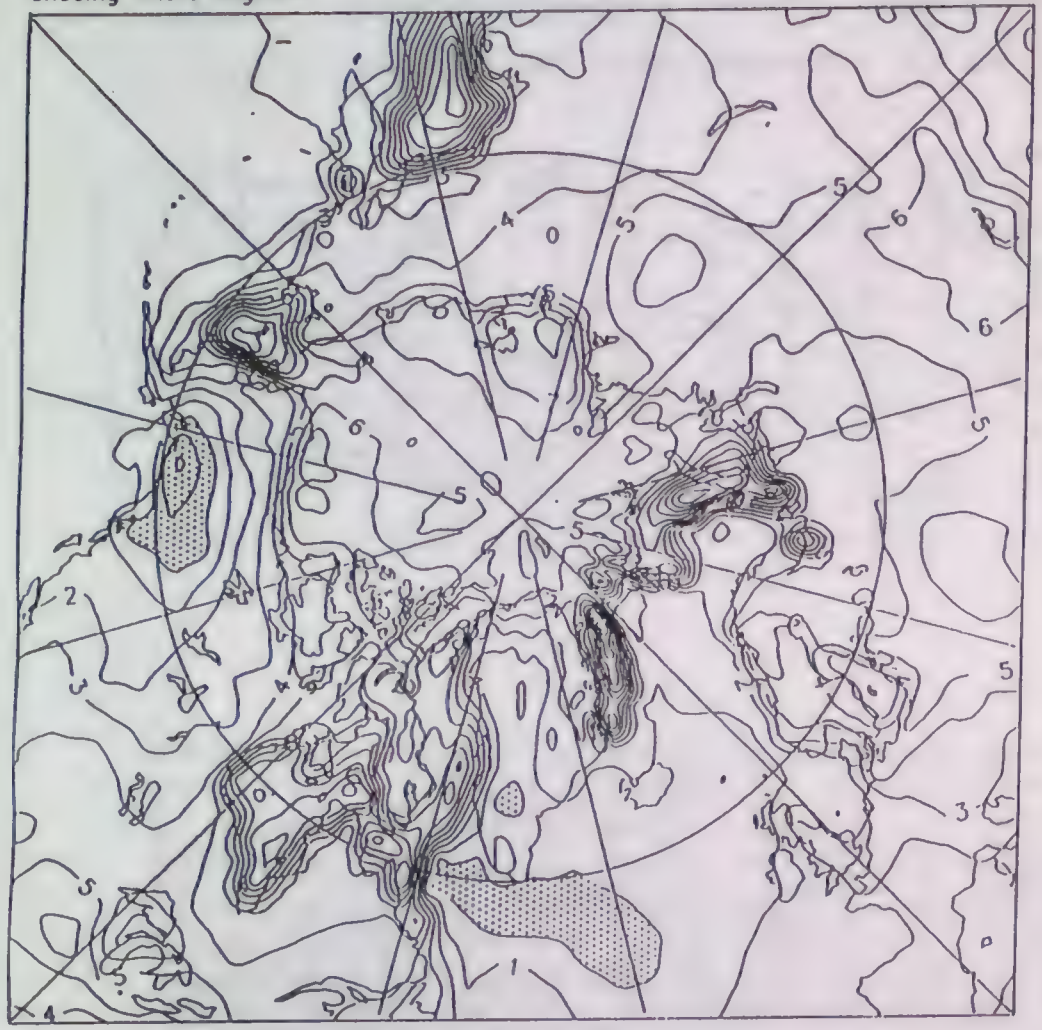

SURFACE TEMPERATURE DIFFERENCE for JJA
transient coupled model: anomaly – control (yrs 66 to 75)
contours at intervals of 1
shading where negative

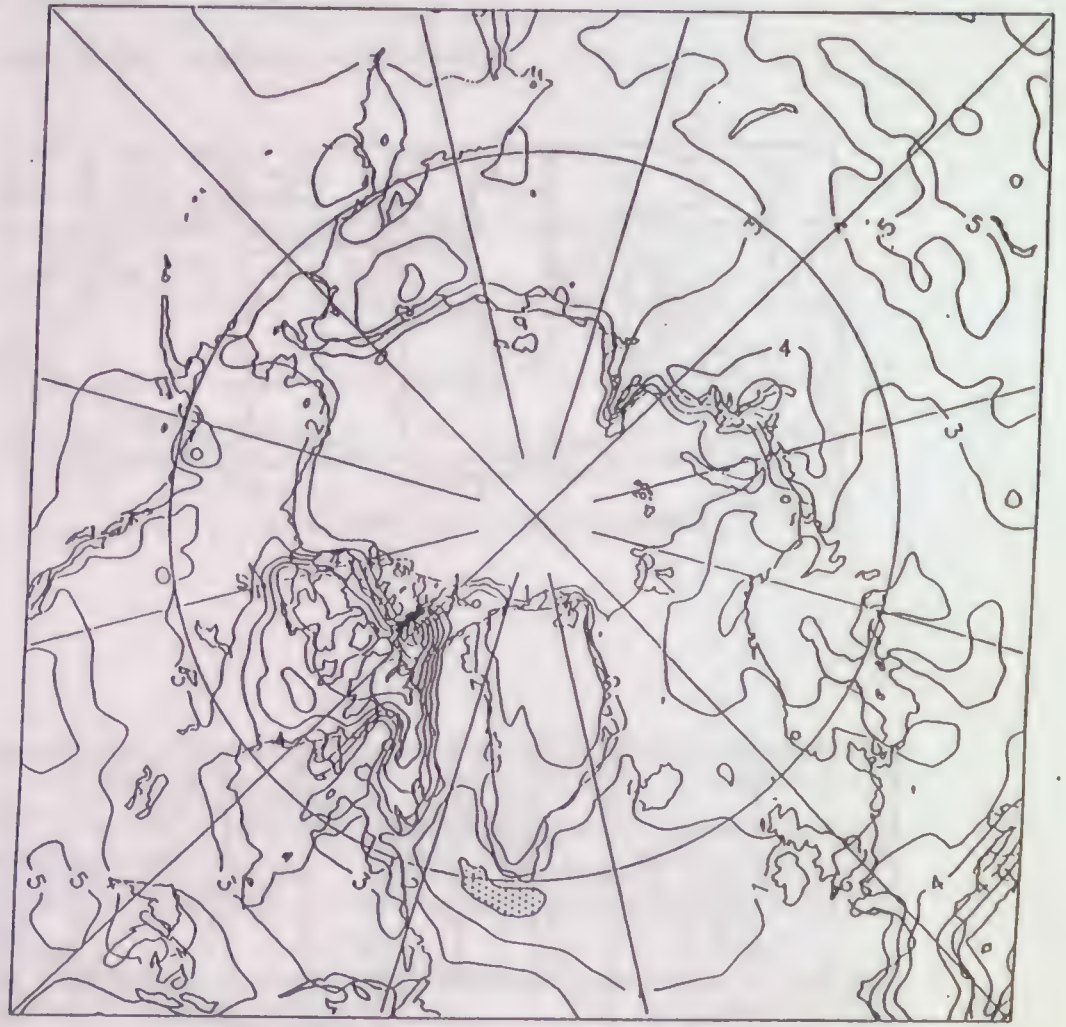

Fig. 3. Unit hPa

PMSL DIFFERENCE for DJF
transient coupled model: anomaly – control (yrs 66 to 75)
contours at intervals of 1
shading where negative

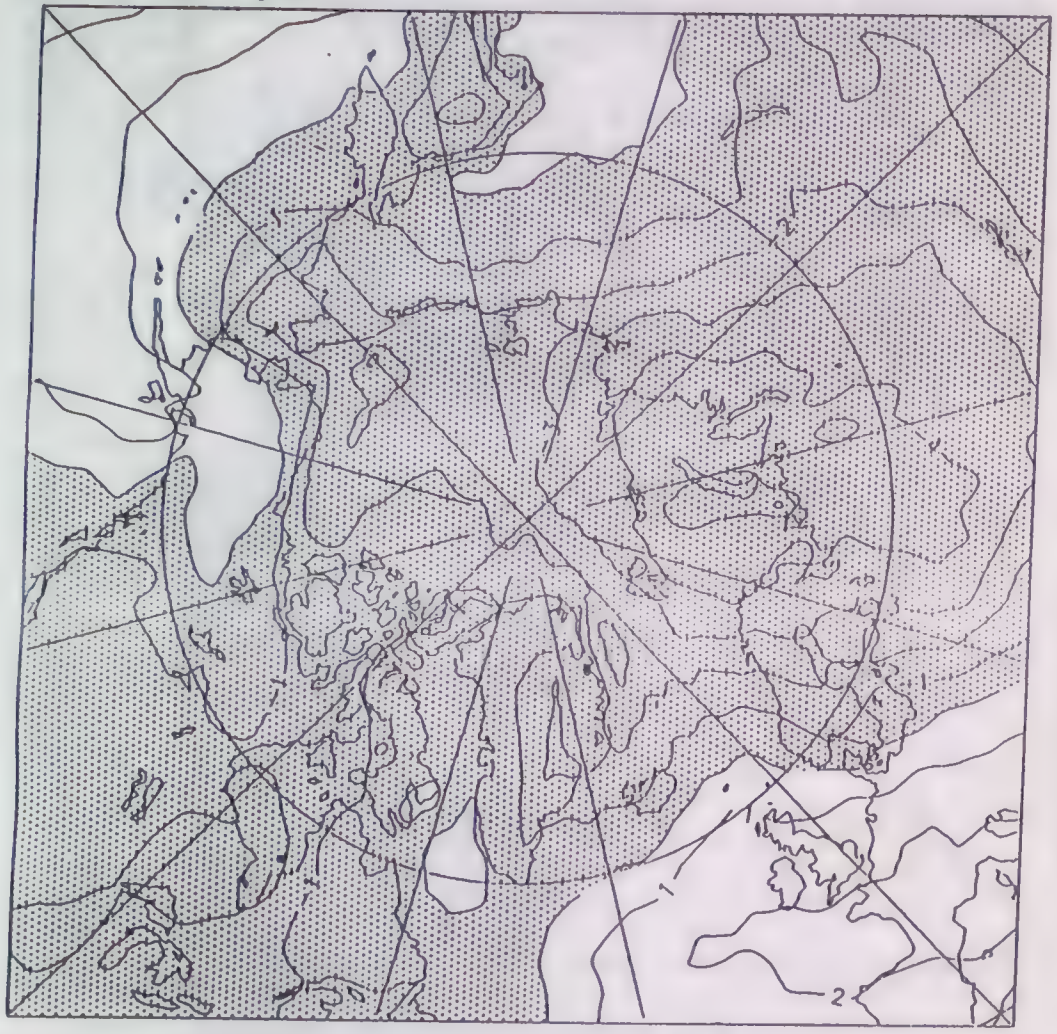

PMSL DIFFERENCE for JJA
transient coupled model: anomaly – control (yrs 66 to 75)
contours at intervals of 1
shading where negative

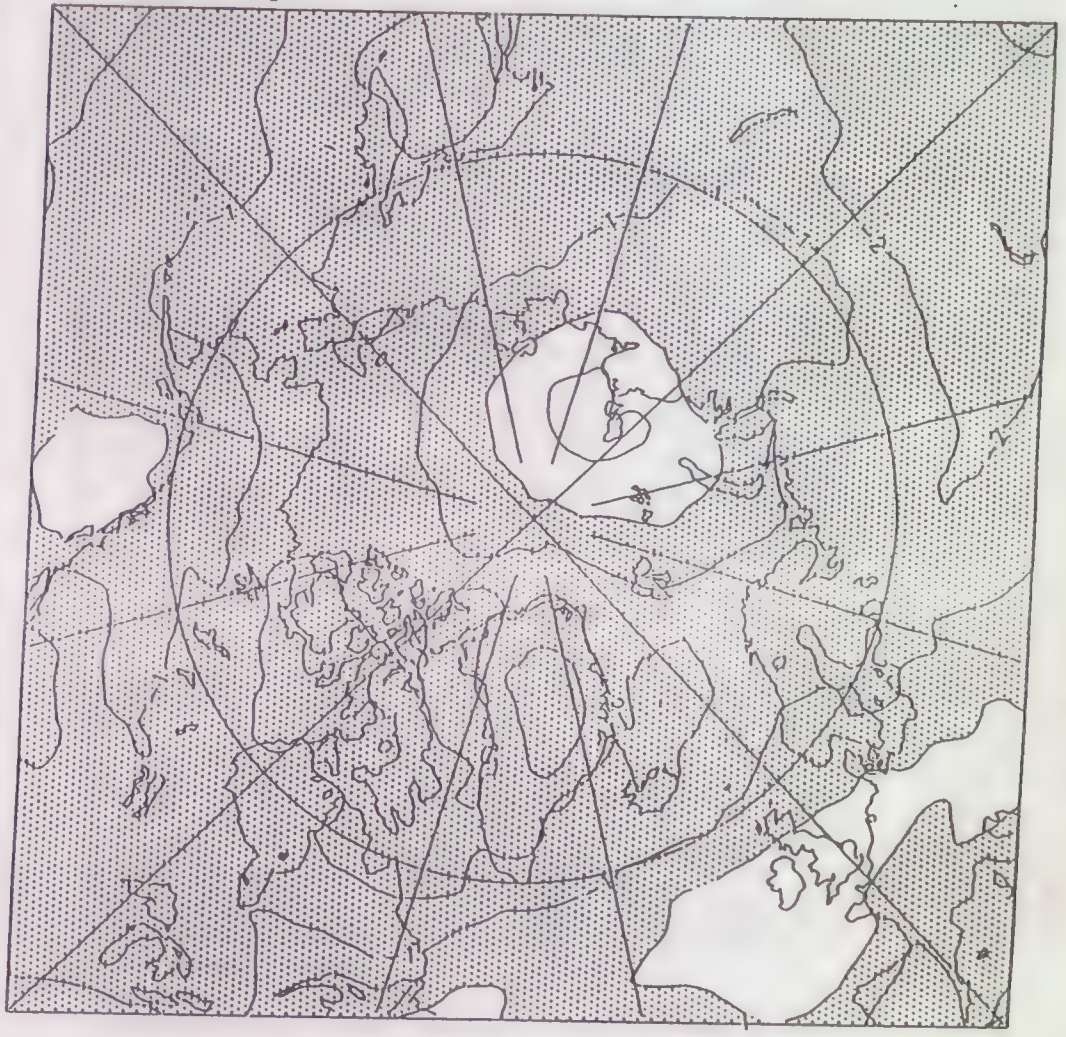

Fig. 4. Unit mm/day

TOTAL PRECIPITATION DIFFERENCE for DJF
transient coupled model: anomaly – control (yrs 66 to 75)
contours at 0,+– 0.25,0.5,0.75,1.0
shading where negative

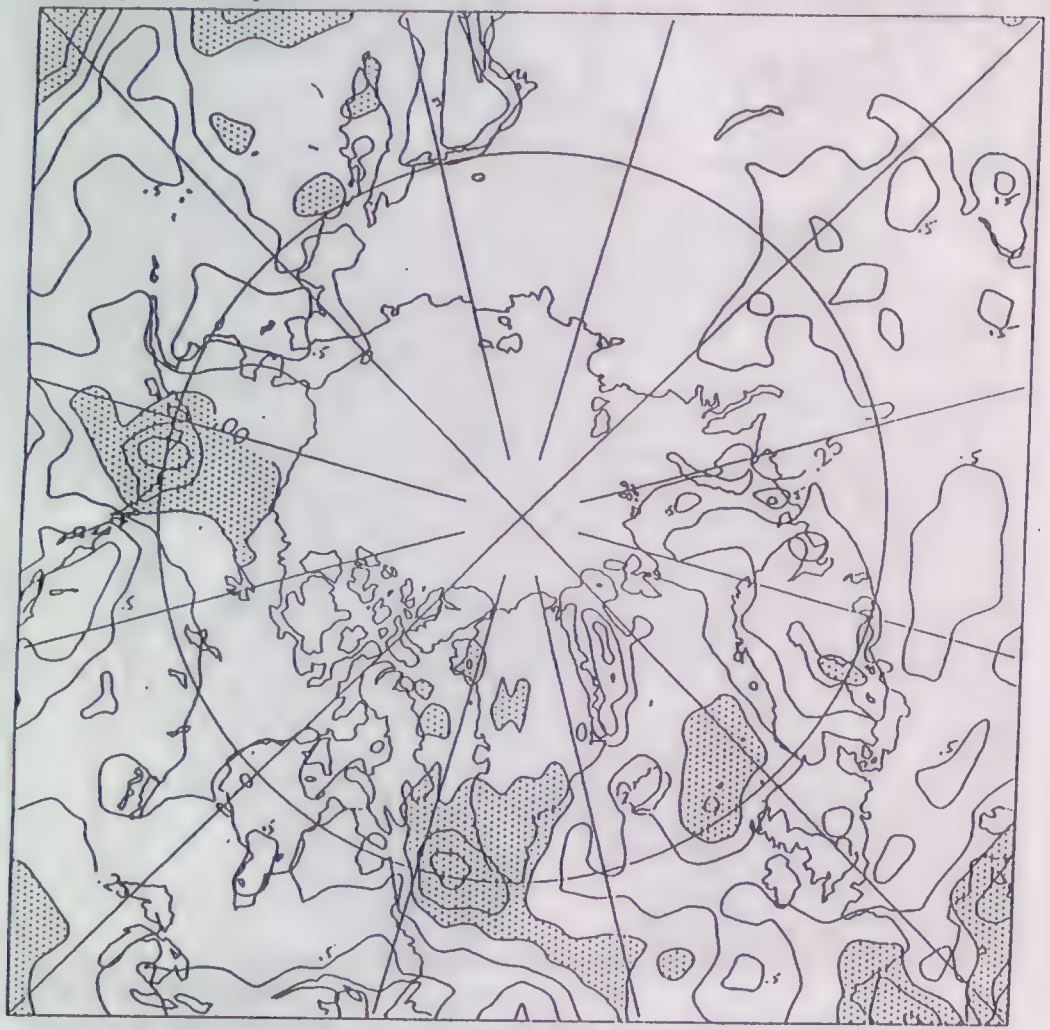

TOTAL PRECIPITATION DIFFERENCE for JJA
transient coupled model: anomaly – control (yrs 66 to 75)
contours at 0,+– 0.25,0.5,0.75,1.0
shading where negative

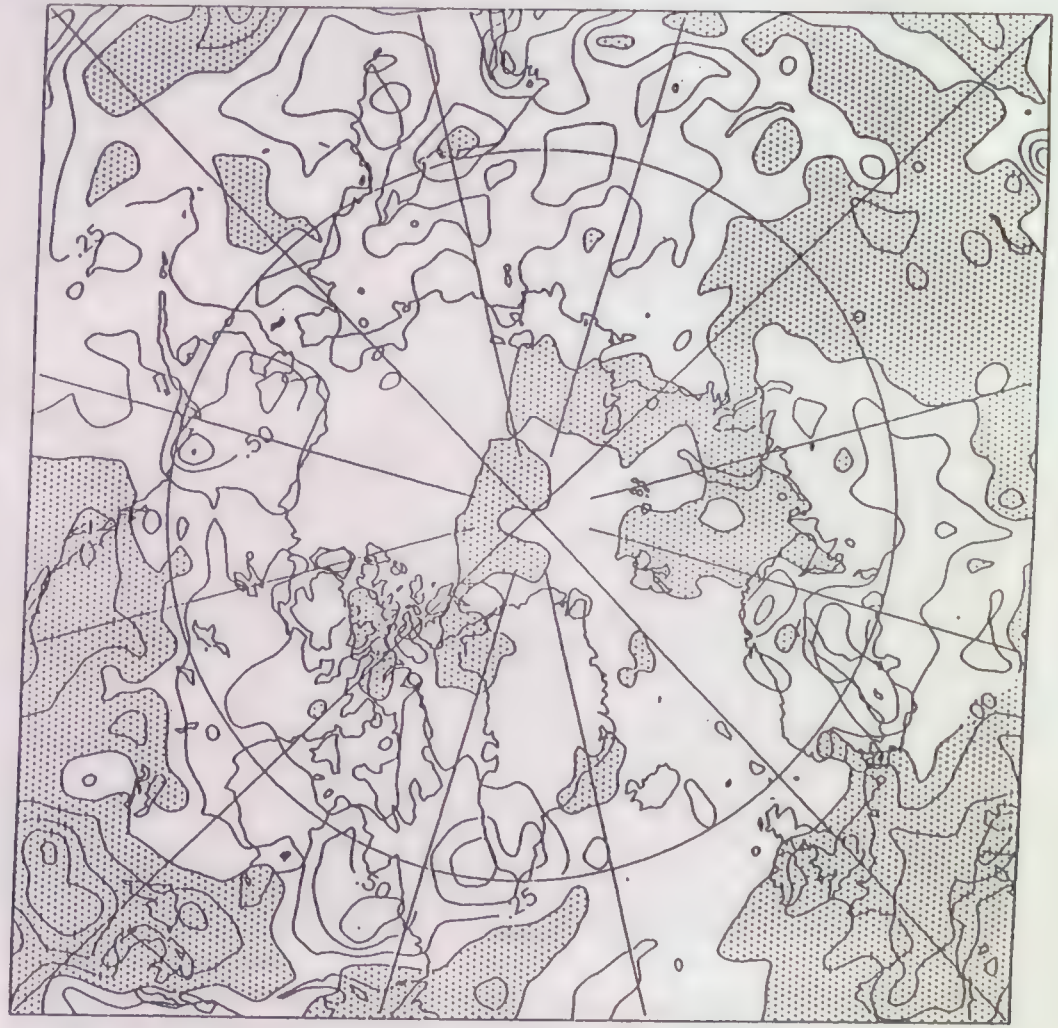

Fig. 5. Soil Moisture (cm)

DIFFERENCE for DJF

transient coupled model: anomaly – control (yrs 66 to 75)
contours at intervals of 1
shading where negative

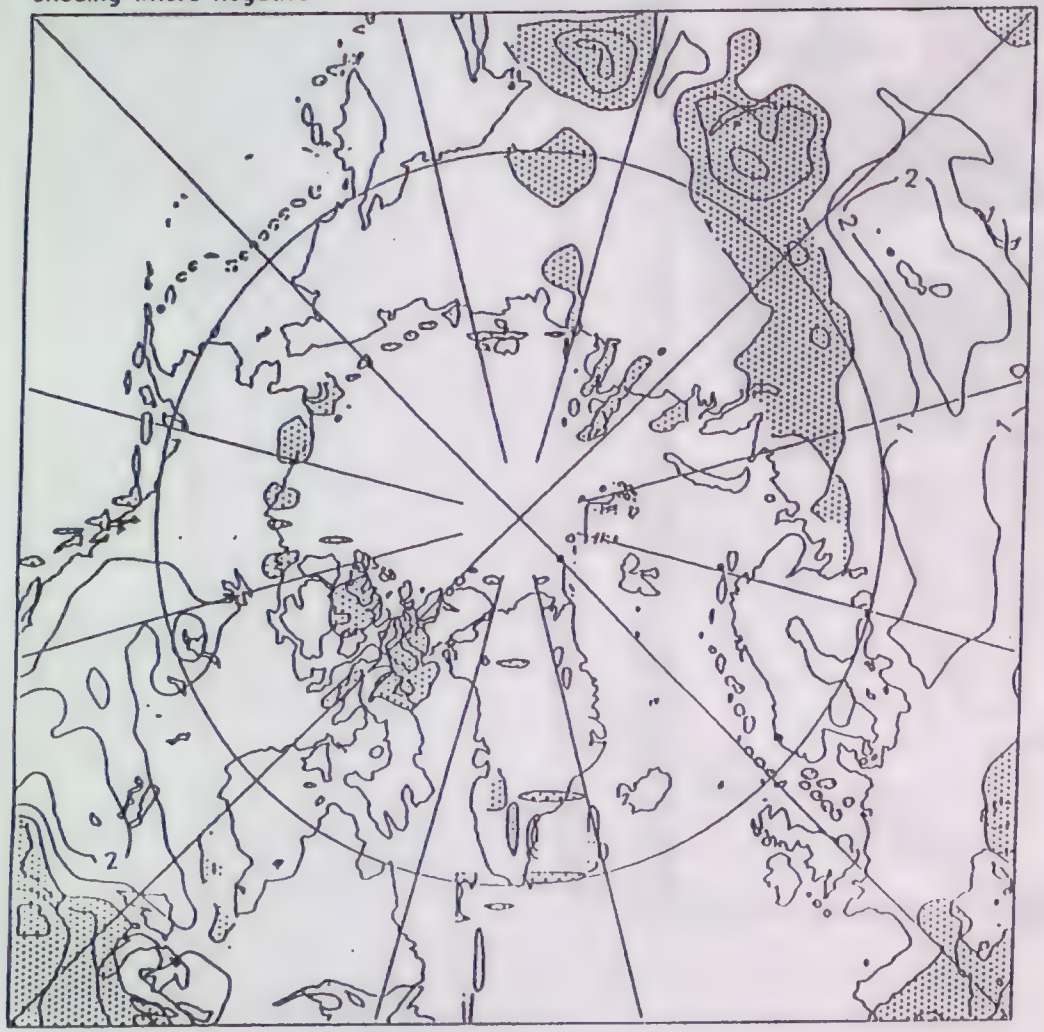

DIFFERENCE for JJA

transient coupled model: anomaly – control (yrs 66 to 75)
contours at intervals of 1
shading where negative

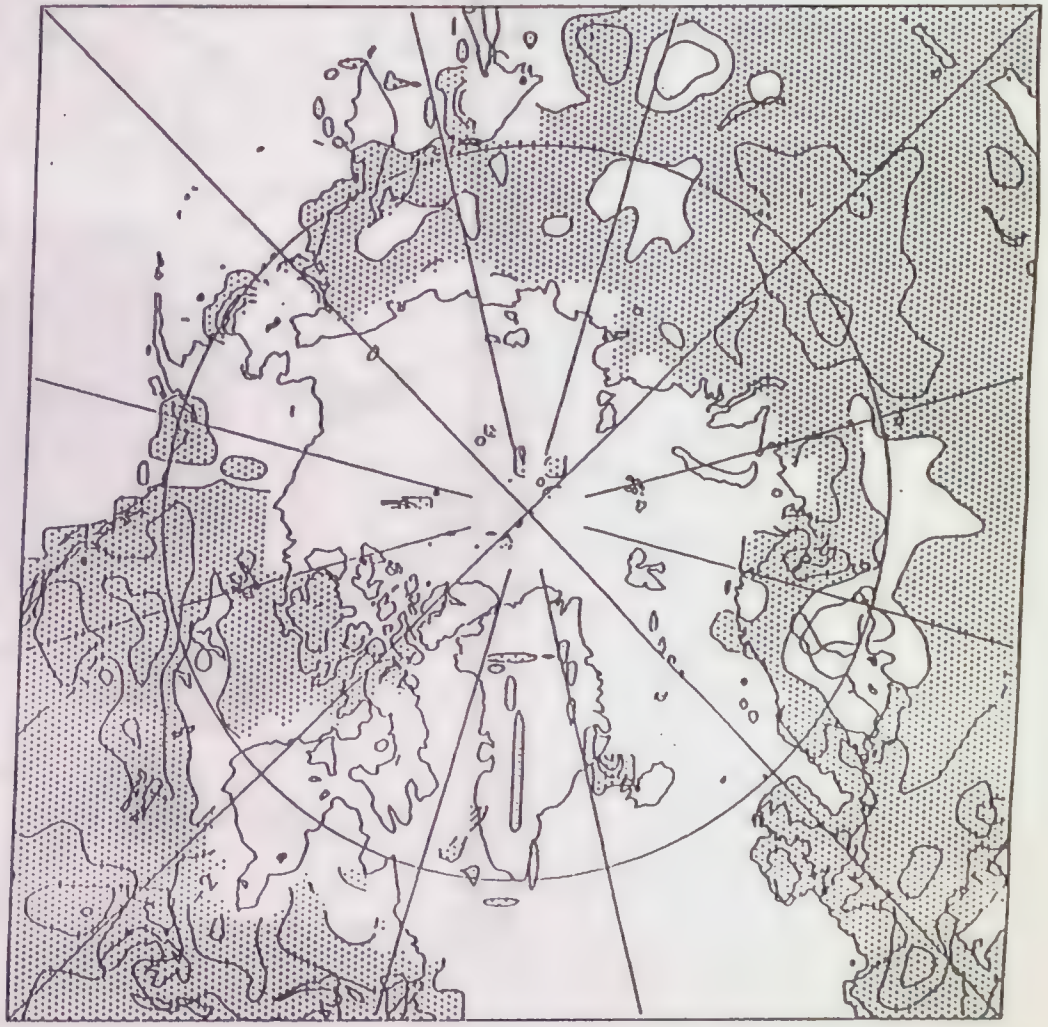

Fig.6. Increase in JJA probability of dry day, years 66-75

Contour interval 0.05, negative regions shaded.

Fig. 7. Unit Kg/m^2

SNOW MASS DIFFERENCE for DJF
transient coupled model: anomaly – control (yrs 66 to 75)
contours 0,+–5,10,20,50,100
shading where negative

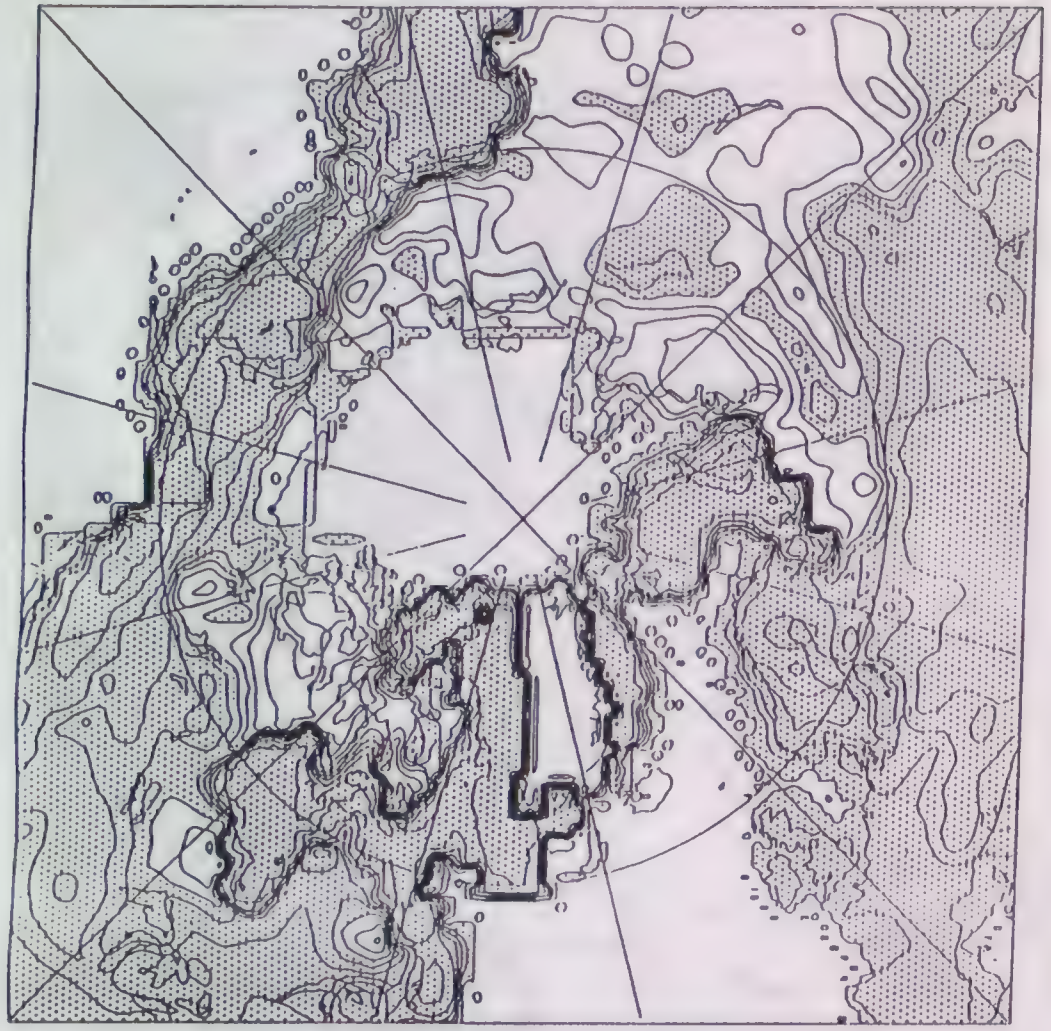

SNOW MASS DIFFERENCE for JJA
transient coupled model: anomaly – control (yrs 66 to 75)
contours 0,+–5,10,20,50,100
shading where negative

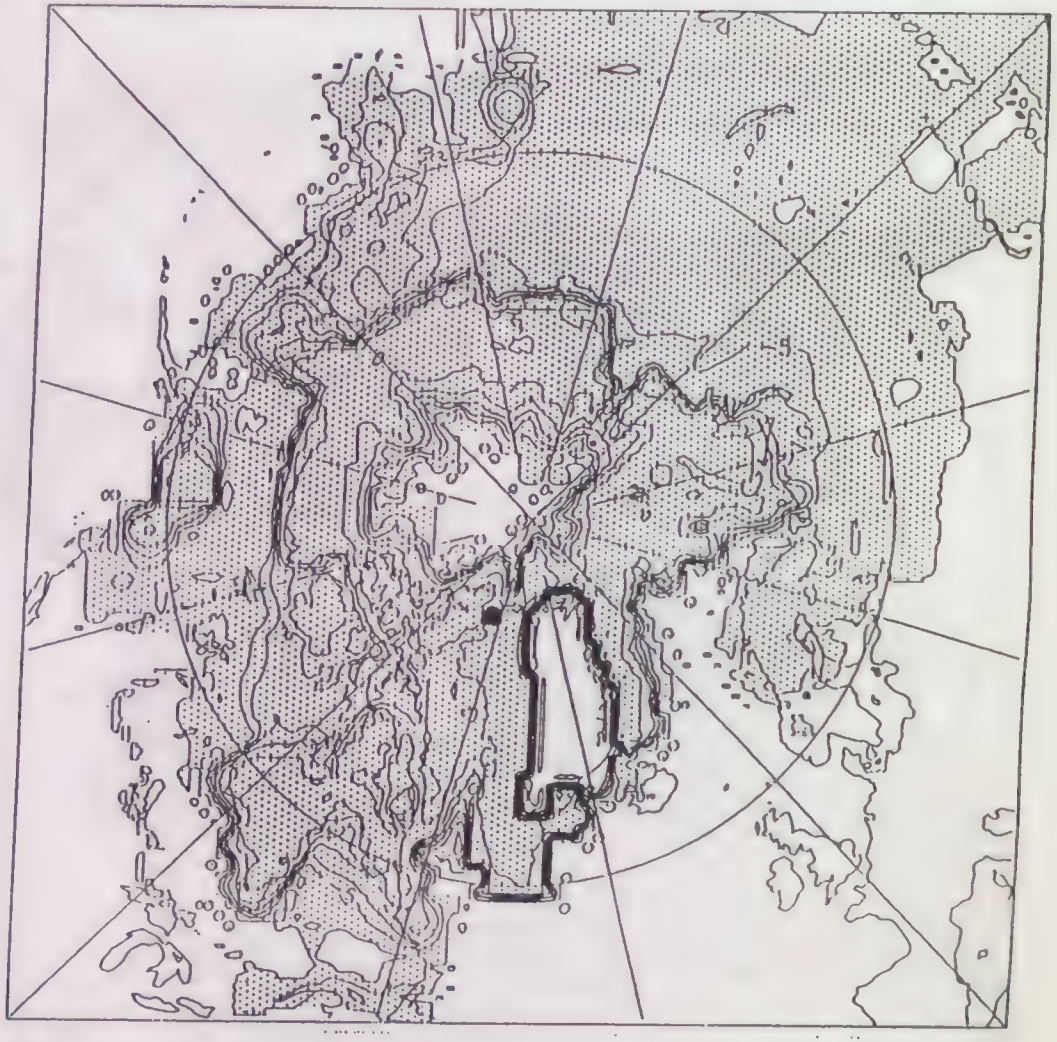

Fig. 8. Unit mm/day (water equivalent)

SNOWFALL DIFFERENCE for DJF
transient coupled model: anomaly – control (yrs 66 to 75)
contours at 0,+– 0.25,0.5,0.75,1.0
shading where negative

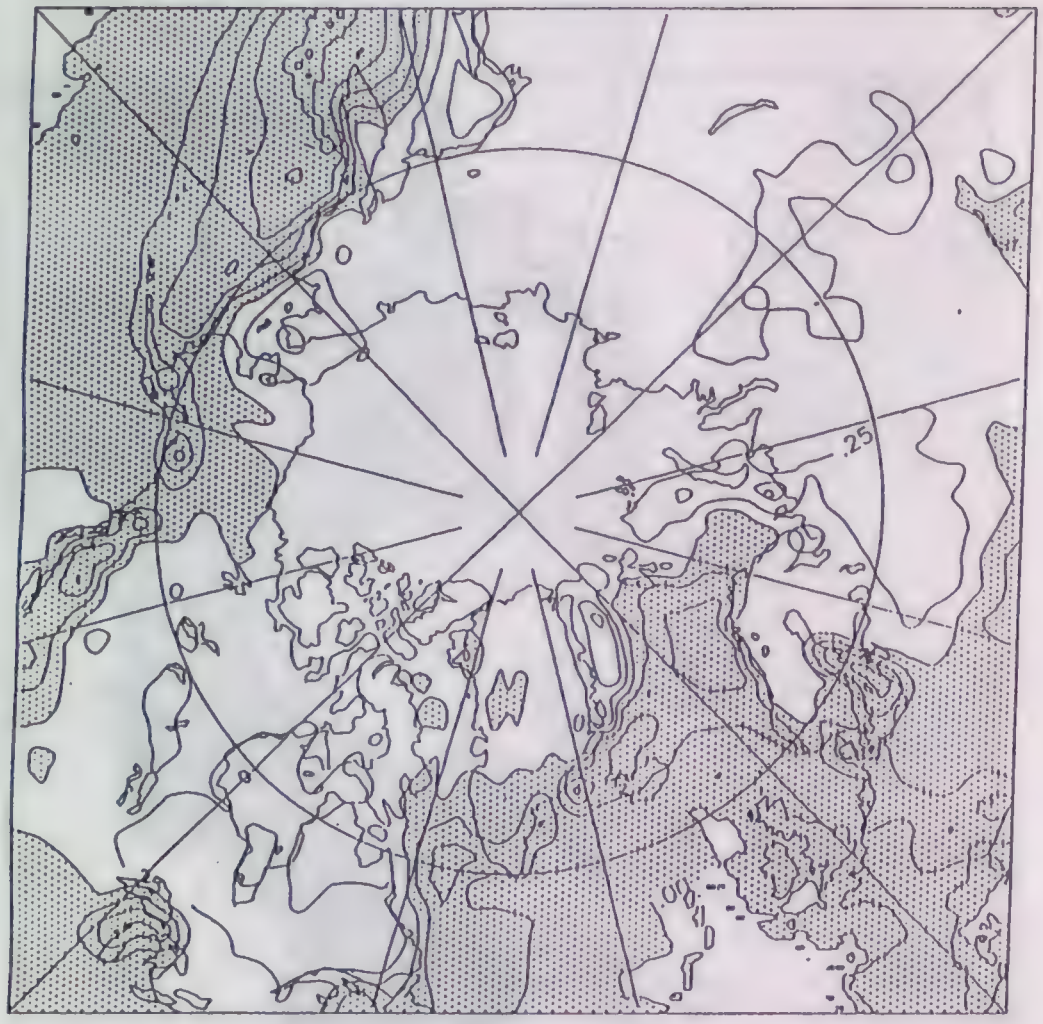

SNOWFALL DIFFERENCE for JJA
transient coupled model: anomaly – control (yrs 66 to 75)
contours at 0,+– 0.25,0.5,0.75,1.0
shading where negative

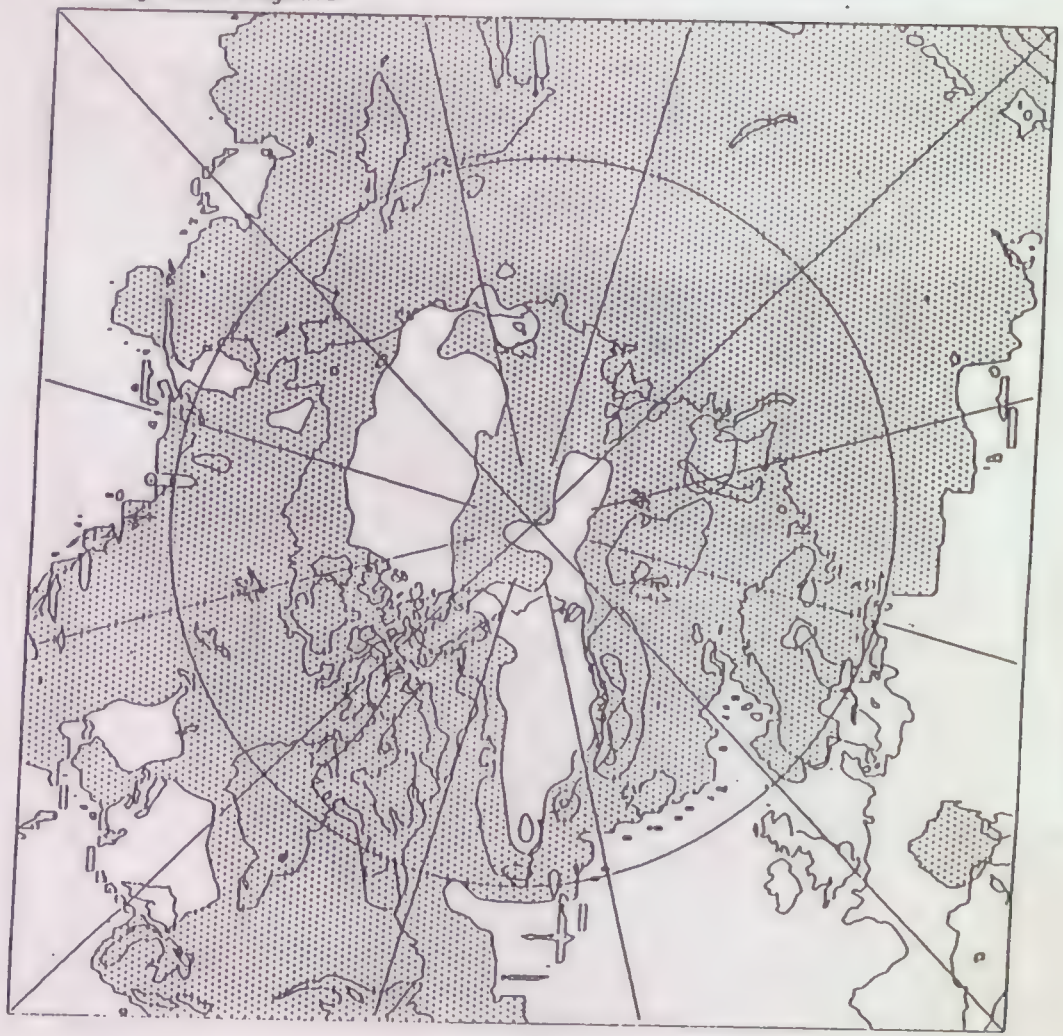

CLIMATE RESEARCH TECHNICAL NOTES

CRTN 1	Oct 1990	Estimates of the sensitivity of climate to vegetation changes using the Penman-Monteith equation. P R Rowntree
CRTN 2	Oct 1990	An ocean general circulation model of the Indian Ocean for hindcasting studies. D J Carrington
CRTN 3	Oct 1990	Simulation of the tropical diurnal cycle in a climate model. D P Rowell
CRTN 4	Oct 1990	Low frequency variability of the oceans. C K Folland, A Colman, D E Parker and A Bevan
CRTN 5	Dec 1990	A comparison of 11-level General Circulation Model Simulations with observations in the East Sahel. K Maskell
CRTN 6	Dec 1990	Climate Change Prediction. J F B Mitchell and Qing-cun Zeng
CRTN 7	Jan 1991	Deforestation of Amazonia - modelling the effects of albedo change. M F Mylne and P R Rowntree
CRTN 8	Jan 1991	The role of observations in climate prediction and research. D J Carson
CRTN 9	Mar 1991	The greenhouse effect and its likely consequences for climate change. D J Carson
CRTN 10	Apr 1991	Use of wind stresses from operational N.W.P. models to force an O.G.C.M. of the Indian Ocean. D J Carrington
CRTN 11	Jun 1991	A new daily Central England Temperature series, 1772-1991. D E Parker, T P Legg and C K Folland
CRTN 12	Jul 1991	Causes and predictability of Sahel rainfall variability. D P Rowell, C K Folland, K Maskell, J A Owen, M N Ward

CLIMATE RESEARCH TECHNICAL NOTES

CRTN 13	Jul 1991	Modelling changes in climate due to enhanced CO2, the role of atmospheric dynamics, cloud and moisture. C A Senior, J F B Mitchell, H Le Treut and Z-X Li
CRTN 14	Sep 1991	Sea temperature bucket models used to correct historical SST data in the Meteorological Office. C K Folland
CRTN 15	Aug 1991	Modelling climate change, and some potential effects on agriculture in the U.K. P R Rowntree, B A Callander and J Cochrane
CRTN 16	Aug 1991	The Boreal Forests and Climate G Thomas and P R Rowntree
CRTN 17	Aug 1991	Development of a Stratosphere-Troposphere Data Assimilation System. R Swinbank.
CRTN 18	Sep 1991	A study of asynchronous coupling using a simple climate model. M K Davey.
CRTN 19	Sep 1991	The Oceanic Carbon Cycle. N K Taylor
CRTN 20	Nov 1991	Worldwide ocean-atmosphere surface fields in Sahel wet and dry years using provisionally corrected surface wind data. M N Ward
CRTN 21	Dec 1991	Coupled tropical ocean global atmosphere models at the UKMO. M K Davey, C Gordon, S Ineson and S Lawrence
CRTN 22	Dec 1991	Empirical parameterisation of tropical ocean-atmosphere coupling. M Allen, M K Davey, D L T Anderson and P D Killworth
CRTN 23	Feb 1992	The temporal evolution of Equatorial Currents in the Indian Ocean D L T Anderson, D J Carrington, R A Corry and C Gordon
CRTN 24	Feb 1992	Stratospheric analyses provided by the U.K. Meteorological Office M J Bailey, A O'Neill and V D Pope

CLIMATE RESEARCH TECHNICAL NOTES

CRTN 25	Feb 1992	Modelling interannual variability in the Indian Ocean using momentum fluxes from the UKMO and ECMWF operational weather analyses. D L T Anderson and D J Carrington
CRTN 26	Mar 1992	A GCM simulation of the impact of Amazonian deforestation on climate using an improved canopy representation J Lean and P R Rowntree
CRTN 27	Mar 1992	The parameterization of rainfall interception in GCMs A J Dolman and D Gregory
CRTN 28	Jun 1992	Development of worldwide marine data eigenvectors since 1985 A W Colman
CRTN 29	Jun 1992	A tropical ocean model with reduced physics M K Davey
CRTN 30	Jun 1992	International Temperature Workshop, Boulder, Colorado, USA, 16 January 1992 Edited by D E Parker
CRTN 31	Jul 1992	Simulation of clear-sky outgoing longwave radiation over the oceans using operational analyses A Slingo and M J Webb
CRTN 32	Sep 1992	A prediction of the transient response of climate J M Murphy
CRTN 33	Nov 1992	LEPS scores for assessing climate model simulations and long-range forecasts. C K Folland
CRTN 34	Jan 1993	Stratospheric Data Assimilation System Guide Editer: R Swinbank
CRTN 35	Mar 1993	A Stratosphere-Troposphere Data Assimilation System R Swinbank and A O'Neill
CRTN 36	Mar 1993	Validation of hydrological schemes for climate models against catchment data. P R Rowntree and J Lean

CLIMATE RESEARCH TECHNICAL NOTES

CRTN 37	Apr 1993	Modelling of palaeoclimates: Examples from the recent past J F B Mitchell
CRTN 38	May 1993	A simulation of seasonality in ENSO forecast skill M K Davey, D L T Anderson and S Lawrence
CRTN 39	Jul 1993	ENSO Prediction experiments using a simple ocean-atmosphere model D-H Wu, D L T Anderson and M K Davey
CRTN 40	Sep 1993	Diagnosis of dynamic sea-surface and sea-level changes from the Cox ocean model J M Gregory
CRTN 41	Sep 1993	Seasonal variations of the clear-sky greenhouse effect: the role of changes in atmospheric temperatures and humidities M J Webb, A Slingo and G L Stephens
CRTN 42	Nov 1993	Sea-level changes under increasing atmospheric CO_2 in a transient coupled ocean-atmosphere GCM experiment. J M Gregory